



RESEARCH ARTICLE

PERFORMANCE EVALUATION of STAGED ORC POWER PLANT SOURCED by WASTE HEAT

İlyas CEYLAN^{1*}, Oğuz ARSLAN²

¹Bilecik Şeyh Edebali University, Faculty of Engineering, Departement of Mechanical Engineering, Bilecik, ilyasceylan1995@gmail.com, ORCID: 0000-0001-5404-1551

²Bilecik Şeyh Edebali University, Faculty of Engineering, Departement of Mechanical Engineering, oguz.arslan@bilecik.edu.tr, ORCID: 0000-0001-8233-831X

Receive Date: 28.02.2022

Accepted Date: 05.05.2022

ABSTRACT

Organic Rankine Cycle (ORC) is a power cycle in which energy can be produced without extra heating. The basic logic is to generate energy with the help of special fluids that can change phase at low temperatures. In this study, one, two and three stage ORC sourced by waste heat was designed and analyzed in view point of different working fluids. In this aim, it was aimed to investigate the stage and fluid effects on the performance of the system. As a result of the study, it was determined that the efficiency increases with increase of the number of stages. It was also determined that the used fluid type was effective on the performance of the staged system. The energy and exergy efficiency of the three-staged ORC was determined as 31% and 49%, respectively.

Keywords: *Energy, Exergy, Staged ORC, Waste heat.*

1. INTRODUCTION

As known, Rankine cycle is a thermodynamic cycle that converts heat energy into work, and water is used as the working fluid of the cycle for many years. Water is a traditional liquid in the Rankine cycle and is the first choice for generating electricity in large and medium power plants. Although it is preferred as a working fluid due to its safety, environmental protection, and high heat transfer properties, it also has some disadvantages. Some of the disadvantages are high abrasiveness and high freezing temperature [1]. In recent years, hydrocarbon-based fluids with a higher molecular weight and lower boiling temperature are used instead of water in the Rankine cycle called as organic Rankine Cycle (ORC). ORCs are sourced by low temperature resources such as waste heat, solar energy and geothermal energy. ORCs have become one of the most common power generation processes depending on the parameters such as climate change, rising oil prices and environmental problems. In this regard, ORC sourced by waste heat is the cleanest and most reliable way for power generation.

In the literature, many studies were conducted about performance of ORCs [2-5], optimization of ORCs [6-10] and heat sources of ORCs [11-13]. The waste heat is one the most preferred energy sources in ORC power plants. Varga et al. [13] investigated the partial replacement of an air cooler to

observe the waste heat behaviour during the temperature decreasing from 140 °C to 45 °C. In this study, they determined that 32 MW of heat released to the environment. Chen et al. [14], developed a mathematical model for the integration of ORC with the circulating heat transfer fluid as an intermediate fluid for the waste heat recovery. In this aim, an ORC-integrated superstructure was proposed that considers all possible heat exchange couplings between waste heat process streams, circulating heat transfer fluid, and ORC. Arslan et al. [15] designed a multiple generation system including electricity generation, domestic hot water and H₂ production for waste recovery of a 150 MW coal-fired power plant. A high-temperature electrolyzer is integrated into the existing system to produce H₂. The second product of O₂ from the electrolyzer was used to enrich the combustion process. The power required for the electrolyzer was obtained from the bottom organic Rankine cycle (ORC). In this context, a supercritical ORC was designed using cyclopentane as the working fluid. An increase of 15.78%–16.53% was achieved in energy efficiency. This increase was achieved in exergy efficiency by 20.43-21.16%. In another study of Arslan [16], supercritical ORC with R601 was investigated. The ORC was sourced by waste heat. The energy and exergy efficiencies of the ORC were recorded as 15.59% and 32.93%, respectively. The kind of the used working fluid is also much important for the system performance of ORC power plants. Arslan et al. [17], investigated s1 type supercritical ORC power plant with an installed capacity of 64.2 MW. They used R744 as the working fluid in the system. They parametrically analyzed the designed system for different temperature and pressures. For the most profitable design, T_{1b}, T_{2a} and P_{2a} were determined as 80 °C, 130 °C and 12 MPa, respectively. Tzu-Chen Hung [18], investigated various working fluids such as Benzene (C₆H₆), Toluene (C₇H₈), p-Xylene (C₈H₁₀), R113, and R123. Among the studied working fluids, p-Xylene has the highest efficiency and Benzene has the lowest efficiency. The study also showed that irreversibilities strongly depend on the type of heat source.

Literature reviews have shown that double loop, triple loop, and multi-loop ORC has better performance in comparison to the single ORC for the recovery of waste heat. Studies showed that using multi-staged ORCs can significantly improve thermal efficiency and heat source utilization rate. One of the most effective ways to improve ORC's performance is to increase the ORC's cycle count. Double-loop ORC (DL-ORC) has shown great potential in thermodynamic and economic performance. In addition, DL-ORC has a low carbon footprint and high CO₂ emission reduction [19,20]. Braimakis et al. [21] investigated the thermo-economic optimization of the ORC-ORC combined power system. They optimized the use of ORC-ORC for waste heat recovery. The researchers aimed to explore the increasing potential of the exergy efficiency for the ORC-ORC combined power system in comparison to a single-stage ORC. The heat source temperature ranging between 100 and 300 °C were investigated. They concluded that the power output and exergy efficiency can be increased by ORC-ORC in comparison to single-stage cycles at the same these operating conditions. Xia et al. [22] performed the working fluid selection for double-loop ORC (DL-ORC) using multi-objective optimization. The targets for optimization are the payback period, annual emission reduction and exergy efficiency. Study results showed that cyclohexane/butane was the most suitable working fluid amongst the 18 candidate working fluid pairs.

In this study, ORC with three loops, sourced by the waste heat of a ceramic production process was performed parametrically. The designed systems were thermodynamically analyzed by energy and exergy methods. In the analyses, EES software was used. Finally, the best designed system was determined in terms of turbine inlet temperature and pressure, and kind of working fluids.

2. MATERIAL AND METHOD

In the most industrial applications, waste heat is discharged to the environment. Especially in the cement and iron and steel industries, a significant amount of waste heat is lost in the form of flue gases at temperatures of 200-300 °C. These temperature levels are not high enough to recover this waste heat through conventional steam Rankine cycles. For this reason, ORC applications are widely used in industrial waste heat recovery applications. In this study, the waste heat of stack gases of the ceramic production process was evaluated in an ORC with tree loops. The data of waste is given in Table 1 [23].

Table 1. Waste heat data used in the study [23].

Flow rate (m^3/h)	16939		
Gas velocity (m/min)	7.4		
Humidity (%)	5.2		
Pressure (kPa)	92.2		
Flow rate(Nm^3/h)	10817		
Dry cond. Flow rate (Nm^3/h)	10258		
	Measurement 1	Measurement 2	Measurement 3
Gas Temp. (°C)	116.0	115.0	117.0
Dust (kg/h)	0.0014	0.0014	0.0015
CO (kg/h)	0.1432	0.1512	0.1751
SO_2 (kg/h)	0.0000	0.0000	0.0182
NO (kg/h)	0.1364	0.1449	0.1535
NO_2 (kg/h)	0.2092	0.2222	0.2353

The type of fluid directly affects the dryness of the steam at the turbine outlet. The slope of the saturated vapour curve of the fluid used in the Rankine cycle is given by ξ value. In this term, the fluid is classified as wet type when ξ value is less than zero. It is named as dry type when ξ value is greater than zero. It is classified as isentropic type when ξ value is equal to zero. In Table 2, the used fluids and its slopes are given.

Table 2. The properties of used refrigerants [24-28].

Fluid	Molecular Weight (g)	Critical Temperature (K)	Critical Pressure (kPa)	ODP	GW P	ξ	Type
R-134a	102.03	374.21	4059	0	1430	-0.39	Wet
R-13	104.46	301.88	3879	1	1440	-3.39	Wet
R-22	86.47	369.3	4990	0.05	1810	-1.33	Wet
R-123	152.93	456.83	3668	0.02	77	0.26	Dry
R-290	44.10	369.83	4200	0	3	-0.79	Wet
R-600	58.12	425.13	3796	0	4	1.03	Dry
R-	58.12	425.17	3800	0	3	1.03	Dry

Fluid	Molecular Weight (g)	Critical Temperature (K)	Critical Pressure (kPa)	ODP	GW P	ξ	Type
600A R-245fa	134.05	427.20	3651	0	1030	0.19	Isentropic

2.1. System Description

In the purpose of the evaluating the waste heat, the ORC with three loops were designed. The flow diagram and $T-s$ diagrams of the proposed system are given in Fig. 1 and Fig. 2, respectively.

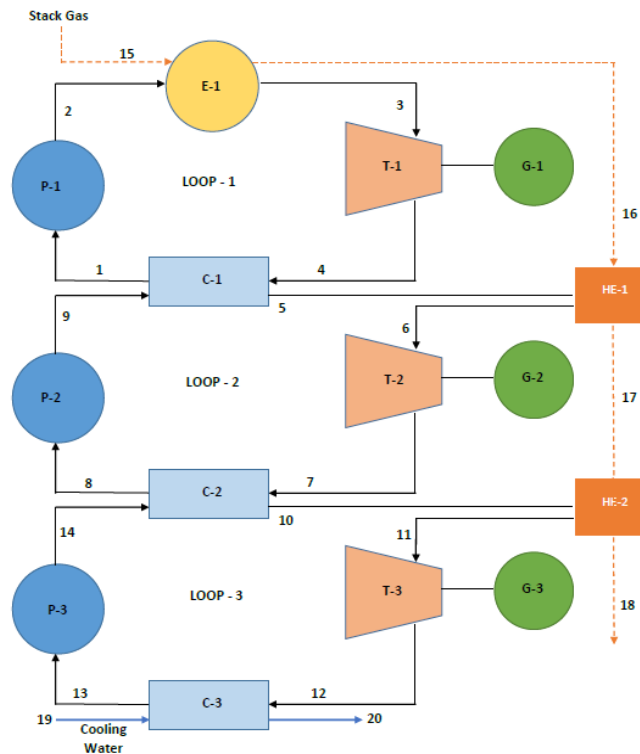


Figure 1. Flow diagram of designed system.

According to Fig 1, the working fluid enters pump 1 (P-1) of the first loop as saturated liquid at point 1 and leaves the pump at point 2. It enters the evaporator 1 (E-1) at the compressed liquid phase, where it draws heat energy from the waste heat source and becomes saturated liquid, then exits E-1. At point 3, the fluid entering the turbine 1 (T/G-1) leaves the T/G-1 as liquid-steam mixture, saturated steam or superheated steam at point 4, depending on the operating conditions. The fluid entering the condenser (C-1) condenses by giving its heat to the fluid in the lower loop.

In the second loop, the fluid enters P-2 as a saturated liquid at point 8 and leaves P-2 at point 9. It enters the condenser of the 1st loop, which is accepted as the pre-heater for the 2nd loop, and takes the waste heat, and enters the heat exchanger 1 (HE-1). In HE-1, the fluid takes the waste heat and leaves

the HE-1 in the saturated vapour phase at point 6. Fluid entering T/G-2 as saturated vapour leaves as superheated steam at point 7. The fluid entering C-2 condenses by giving its heat to the fluid in the 3rd loop, and enters P-2 again as a saturated liquid.

In the third loop, the fluid enters P-3 as a saturated liquid at point 13 and leaves P-3 at point 14. It enters the condenser of the 2nd loop, which is accepted as the pre-heater for the 3rd loop, and takes the waste heat, and enters to HE-2. In HE-2, the fluid takes the waste heat from and leaves the HE-2 in the saturated vapour phase at point 11. The fluid that enters T/G-3 as saturated vapour leaves as superheated vapour. The fluid entering the C-3 condenses by giving its heat to the cooling water.

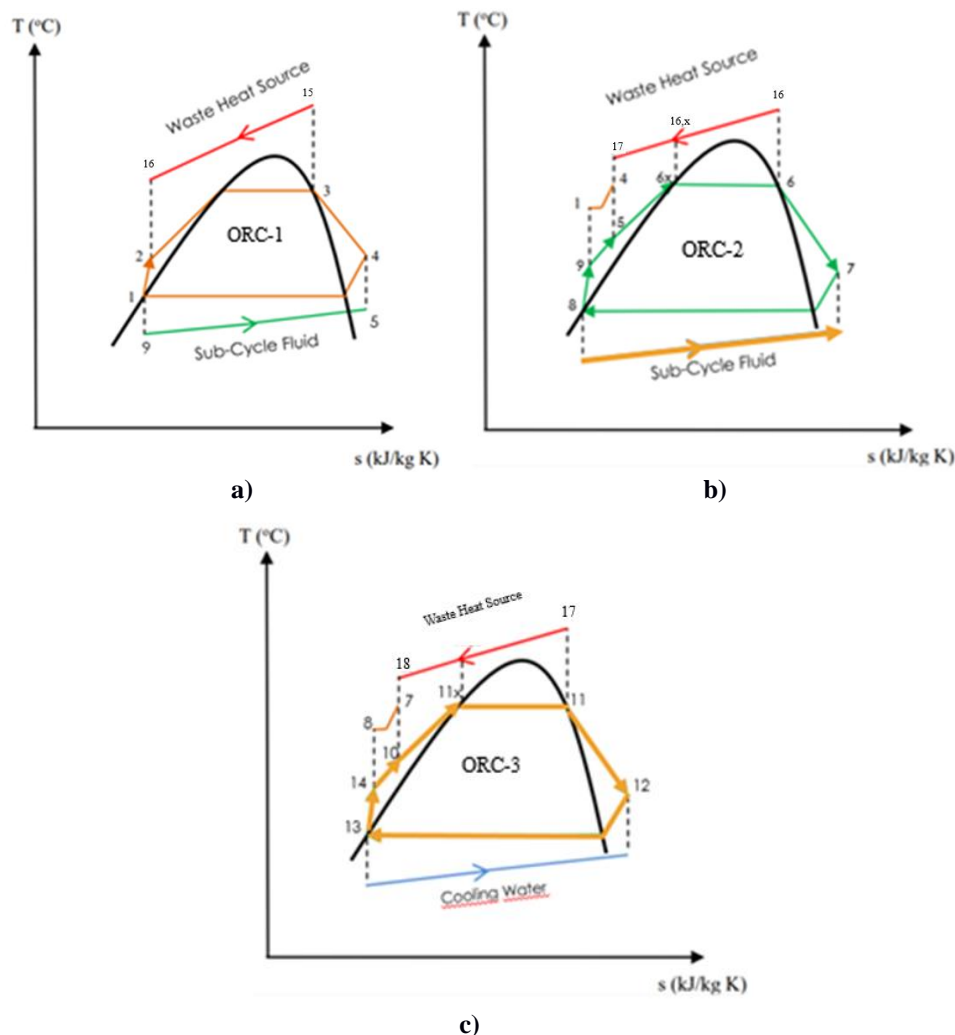


Figure 2. T-s graph of single loop (a) dual loop (b), and triple loop (c).

2.2. Energy Analysis

The conservation of mass and energy is the base of energy analysis. The mass balance, energy balance and energy efficiency equations are given as follows [29]:

$$\sum \dot{m}_{in} = \sum \dot{m}_{out} \quad (1)$$

$$\dot{Q} + \dot{W} = \sum \dot{m}_{out} \dot{h}_{out} - \sum \dot{m}_{in} \dot{h}_{in} \quad (2)$$

$$n_{th} = \frac{\dot{W}_{net}}{\dot{Q}_{net}} \quad (3)$$

The energy balances of the components of the proposed system are given in Table 3.

Table 3. The mass, energy and efficiency equations of the proposed system.

Component	Mass balance	Energy balance	Energy efficiency
E-1	\dot{m}_2 $= \dot{m}_3$ \dot{m}_{15} $= \dot{m}_{16}$	\dot{Q}_{E-1} $= \dot{m}(h_3 - h_2)$	$n_{E-1} = \frac{h_3}{h_2}$
T/G-1	\dot{m}_3 $= \dot{m}_4$	\dot{W}_{T-1} $= \frac{\dot{m}(h_3 - h_4)}{n_{T-1}}$	$n_{T-1} = \frac{h_4}{h_3}$
C-1	\dot{m}_4 $= \dot{m}_1$ \dot{m}_9 $= \dot{m}_5$	\dot{Q}_{C-1} $= \dot{m}(h_4 - h_1)$	$n_{C-1} = \frac{h_1}{h_4}$
P-1	\dot{m}_1 $= \dot{m}_2$	\dot{W}_{P-1} $= \frac{\dot{m}(h_2 - h_1)}{n_{P-1}}$	$n_{P-1} = \frac{h_2}{h_1}$
Loop-1	-	$(\dot{Q}_{E-1} - \dot{Q}_{C-1})$ $- (\dot{W}_{T-1}$ $- \dot{W}_{P-1}) = 0$	$n_{th} = \frac{\dot{W}_{T-1} - \dot{W}_{P-1}}{\dot{m}(h_3 - h_2)}$
HE-1	\dot{m}_{16} $= \dot{m}_{17}$ \dot{m}_5 $= \dot{m}_6$	\dot{Q}_{HE-1} $= \dot{m}(h_6 - h_5)$ $+ \dot{m}(h_{17} - h_{16})$	$n_{HE-1} = \frac{h_6 + h_{17}}{h_5 + h_{15}}$
T/G-2	\dot{m}_6 $= \dot{m}_7$	\dot{W}_{T-2} $= \frac{\dot{m}(h_6 - h_7)}{n_{T-2}}$	$n_{T-2} = \frac{h_7}{h_6}$
C-2	\dot{m}_7 $= \dot{m}_8$ \dot{m}_{14} $= \dot{m}_{10}$	\dot{Q}_{C-2} $= \dot{m}(h_7 - h_8)$	$n_{C-2} = \frac{h_8}{h_7}$

P-2	\dot{m}_8 $= \dot{m}_9$	\dot{W}_{P-2} $= \frac{\dot{m}(h_9 - h_8)}{n_{P-2}}$	$n_{P-2} = \frac{h_9}{h_8}$
Loop-2	-	$(\dot{Q}_{HE-1} - \dot{Q}_{C-2})$ $- (\dot{W}_{T-2}$ $- \dot{W}_{P-2}) = 0$	$n_{th} = \frac{\dot{W}_{T-2} - \dot{W}_{P-2}}{\dot{m}(h_6 - h_5)}$
HE-2	\dot{m}_{17} $= \dot{m}_{18}$ \dot{m}_{10} $= \dot{m}_{11}$	\dot{Q}_{HE-2} $= \dot{m}(h_{11} - h_{10})$	$n_{HE-2} = \frac{h_{11} + h_{18}}{h_{10} + h_{17}}$
T/G-3	\dot{m}_{11} $= \dot{m}_{12}$	\dot{W}_{T-3} $= \frac{\dot{m}(h_{11} - h_{12})}{n_{T-3}}$	$n_{T-3} = \frac{h_{12}}{h_{11}}$
C-3	\dot{m}_{13} $= \dot{m}_{12}$ \dot{m}_{19} $= \dot{m}_{20}$	\dot{Q}_{C-3} $= \dot{m}(h_{13} - h_{12})$	$n_{C-3} = \frac{h_{13}}{h_{12}}$
P-3	\dot{m}_{13} $= \dot{m}_{14}$	\dot{W}_{P-3} $= \frac{\dot{m}(h_{14} - h_{13})}{n_{P-3}}$	$n_{P-3} = \frac{h_{14}}{h_{13}}$
Loop-3	-	$(\dot{Q}_{HE-2} - \dot{Q}_{C-3})$ $- (\dot{W}_{T-3}$ $- \dot{W}_{P-3}) = 0$	$n_{th} = \frac{\dot{W}_{T-3} - \dot{W}_{P-3}}{\dot{m}(h_{11} - h_{10})}$
Overall	-	$[(\dot{Q}_{E-1} + \dot{Q}_{HE-2}$ $+ \dot{Q}_{HE-3}) - (\dot{Q}_{C-1}$ $+ \dot{Q}_{C-2} + \dot{Q}_{C-3})]$ $- [(\dot{W}_{T-1} + \dot{W}_{T-2}$ $+ \dot{W}_{T-3}) - (\dot{W}_{P-1}$ $+ \dot{W}_{P-2} + \dot{W}_{P-3})]$ $= 0$	$n_{th} = \frac{(\dot{W}_{T-1} + \dot{W}_{T-2} + \dot{W}_{T-3}) - (\dot{W}_{P-1} + \dot{W}_{P-2} + \dot{W}_{P-3})}{\dot{m}(h_{15} - h_{18})}$

In the analysis % is the efficiencies of the pumps, turbines and all heat exchangers were included in to calculations as 85%, 85% and 98%, respectively [11].

2.3. Exergy Analysis

Where the first law deals with energy balance, second law deals with irreversibility, entropy generation, and further exergy analysis. The exergy balance and exergy efficiency of the k^{th} component is given as follows [29]:

$$\dot{E}x_{d,k} = \dot{E}x_k^Q + \dot{E}x_k^W + \sum \dot{m}_k \psi_i - \sum \dot{m}_k \psi_{out} \quad (4)$$

where $\dot{E}x_k^Q$, $\dot{E}x_k^W$ and ψ_i respectively indicate the exergy of heat exergy, exergy of work and specific flow exergy. They are given as follows [29]:

$$\dot{E}x_k^Q = \sum (1 - \frac{T_0}{T}) \dot{Q} \quad (5)$$

$$\dot{E}x_k^W = \sum \dot{W} \quad (6)$$

$$\psi_i = (h_i - h_0) - T_0(s_i - s_0) \quad (7)$$

$$\varepsilon_k = 1 - \frac{\dot{E}x_{d,k}}{\dot{E}x_{in,k}} \quad (8)$$

The exergy balances of the components of the proposed system are given in Table 4.

Table 4. The exergy balance equations of the proposed system.

Component	Exergy balance	Exergy efficiency
E-1	$\dot{E}x_{d,E-1} = (\dot{m}_2\psi_2 + \dot{m}_{15}\psi_{15}) - (\dot{m}_3\psi_3 + \dot{m}_{16}\psi_{16} + \sum \dot{Q}_{E-1} (1 - \frac{T_0}{T}))$	$n_{E-1} = \frac{\dot{E}_3 - \dot{E}_2}{\dot{E}_{15} - \dot{E}_{16}}$
T/G-1	$\dot{E}x_{d,T/G-1} = (\dot{m}_3\psi_3) - (\dot{m}_4\psi_4 + \sum \dot{W}_{k,T/G-1})$	$n_{T/G-1} = \frac{\dot{W}_{T/G-1}}{\dot{E}_3 - \dot{E}_4}$
C-1	$\dot{E}x_{d,C-1} = (\dot{m}_4\psi_4 + \dot{m}_9\psi_9) - (\dot{m}_5\psi_5 + \dot{m}_1\psi_1)$	$n_{C-1} = \frac{\dot{E}_1 - \dot{E}_4}{\dot{E}_9 - \dot{E}_5}$
P-1	$\dot{E}x_{d,P-1} = \dot{m}_1\psi_1 - \dot{m}_2\psi_2 + \sum \dot{W}_{k,P-1}$	$n_{P-1} = \frac{\dot{E}_1 - \dot{E}_2}{\dot{W}_{P-1}}$
Loop-1	$\dot{E}x_{d,E-1} + \dot{E}x_{d,T/G-1} + \dot{E}x_{d,C-1} + \dot{E}x_{d,P-1}$	$n_{th} = \frac{\dot{W}_{T/G-1} - \dot{W}_{P-1}}{\dot{E}_{15} - \dot{E}_{16}}$
HE-1	$\dot{E}x_{d,HE-1} = (\dot{m}_{16}\psi_{16} + \dot{m}_5\psi_5) - (\dot{m}_{17}\psi_{17} + \dot{m}_6\psi_6 + \sum \dot{Q}_{HE-1} (1 - \frac{T_0}{T}))$	$n_{HE-1} = \frac{\dot{E}_6 - \dot{E}_5}{\dot{E}_{17} - \dot{E}_{16}}$
T/G-2	$\dot{E}x_{d,T/G-2} = (\dot{m}_6\psi_6) - (\dot{m}_7\psi_7 + \sum \dot{W}_{k,T/G-2})$	$n_{T/G-2} = \frac{\dot{W}_{T/G-2}}{\dot{E}_6 - \dot{E}_7}$
C-2	$\dot{E}x_{d,C-2} = (\dot{m}_{14}\psi_{14} + \dot{m}_7\psi_7) - (\dot{m}_8\psi_8 + \dot{m}_{10}\psi_{10})$	$n_{C-2} = \frac{\dot{E}_8 - \dot{E}_7}{\dot{E}_{14} - \dot{E}_{10}}$
P-2	$\dot{E}x_{d,P-2} = \dot{m}_8\psi_8 - \dot{m}_9\psi_9 + \sum \dot{W}_{k,P-2}$	$n_{P-2} = \frac{\dot{E}_8 - \dot{E}_9}{\dot{W}_{P-2}}$
Loop-2	$\dot{E}x_{d,HE-2} + \dot{E}x_{d,T/G-2} + \dot{E}x_{d,C-2} + \dot{E}x_{d,P-2}$	$n_{th} = \frac{\dot{W}_{T/G-2} - \dot{W}_{P-2}}{\dot{E}_{16} - \dot{E}_{17}}$
HE-2	$\dot{E}x_{d,HE-2} = (\dot{m}_{17}\psi_{17} + \dot{m}_{10}\psi_{10}) - (\dot{m}_{18}\psi_{18} + \dot{m}_{11}\psi_{11} + \sum \dot{Q}_{HE-2} (1 - \frac{T_0}{T}))$	$n_{HE-2} = \frac{\dot{E}_{11} - \dot{E}_{10}}{\dot{E}_{18} - \dot{E}_{17}}$

T/G-3	$\dot{E}x_{d,T/G-3} = (\dot{m}_{11}\psi_{11}) - (\dot{m}_{12}\psi_{12} + \sum \dot{W}_{k,T/G-3})$	$n_{T/G-3} = \frac{\dot{W}_{T/G-3}}{\dot{E}_{11} - \dot{E}_{12}}$
C-3	$\dot{E}x_{d,C-3} = (\dot{m}_{19}\psi_{19} + \dot{m}_{12}\psi_{12}) - (\dot{m}_{13}\psi_{13} + \dot{m}_{20}\psi_{20})$	$n_{C-3} = \frac{\dot{E}_{13} - \dot{E}_{12}}{\dot{E}_{19} - \dot{E}_{20}}$
P-3	$\dot{E}x_{d,P-3} = \dot{m}_{13}\psi_{13} - \dot{m}_{14}\psi_{14} + \sum \dot{W}_{k,P-3}$	$n_{P-3} = \frac{\dot{E}_{13} - \dot{E}_{14}}{\dot{W}_{P-3}}$
Loop-3	$\dot{E}x_{d,HE-3} + \dot{E}x_{d,T/G-3} + \dot{E}x_{d,C-3} + \dot{E}x_{d,P-3}$	$n_{th} = \frac{\dot{W}_{T/G-3} - \dot{W}_{P-3}}{\dot{E}_{17} - \dot{E}_{18}}$
Overall	$\dot{E}x_d = \sum \dot{E}x_{d,k}$	$n_{th} = \frac{\sum \dot{W}_{T/G} - \sum \dot{W}_P}{\dot{E}_{15} - \dot{E}_{18}}$

3. RESULT

The parametric analyses were conducted to evaluate the performance of the proposed system. The used parameters are given in Table 5.

Table 5. The design parameters of the proposed system.

Fixed values	Temperature of waste heat	185 °C – 207 °C
	Coolant Temperature	27 °C
	Condenser Inlet Pressure	900 kPa
Independent variables	Organic Fluids	R290, R123,R134a,R13,R245fa;R600,R600a R22,
	Turbine Inlet Pressure Range	1200 kPa to 2500kPa
	Turbine Inlet Temperature Range	65°C to 80 °C

3.1. The Results of Energy Analysis

The selected fluids were analyzed by energy method. The obtained results are given in Table 6. In Table 6, the fluids were evaluated to determine the available selections as the first decision.

Table 6. Energy efficiency values of the proposed system for the first decision stage.

Temp.	R134A	R13	R22	R123	R245FA	R290	R600	R600a
65 °C	21.45%	0.83%	12.51%	19.97%	19.39%	14.48%	19.62%	19.60%
67 °C	23.06%	0.86%	14.35%	20.04%	19.45%	18.70%	19.70%	19.69%
68 °C	24.46%	0.89%	18.49%	20.12%	19.51%	20.44%	19.78%	19.77%
70 °C	25.69%	0.92%	20.10%	20.19%	19.57%	21.98%	19.86%	19.85%
72 °C	26.67%	0.95%	21.54%	20.26%	19.64%	23.35%	19.93%	19.93%
73 °C	27.73%	0.98%	22.85%	20.33%	19.70%	24.58%	20.01%	20.01%
75 °C	28.57%	1.91%	24.03%	20.40%	19.76%	25.69%	20.09%	20.09%
77 °C	29.32%	3.34%	25.11%	20.48%	19.82%	26.68%	20.16%	20.17%

Temp.	R134A	R13	R22	R123	R245FA	R290	R600	R600a
78 °C	28.95%	4.66%	26.10%	20.55%	19.88%	27.57%	20.24%	20.25%
80 °C	20.34%	5.89%	27.00%	20.62%	19.94%	28.38%	20.32%	20.33%

According to Table 6, the calculations were made for various organic fluids and the three most efficient were selected for analysis of looped system. These fluids were determined as R290, R13, and R123.

3.2. The Case of R290 Use in Each Cycle

In the first stage of the analysis, the calculations were made by using the most efficient fluid of R290 in single, dual, and triple looped cases. First, the ORC with single loop is evaluated. Then, dual and triple looped cases were handled. For the turbine inlet temperature, a temperature difference of 5 °C was taken into account for each loop. The inlet pressure was taken as 2500 kPa. Fig. 3 shows the cycle efficiencies according to the variation of the turbine inlet temperature (T_3).

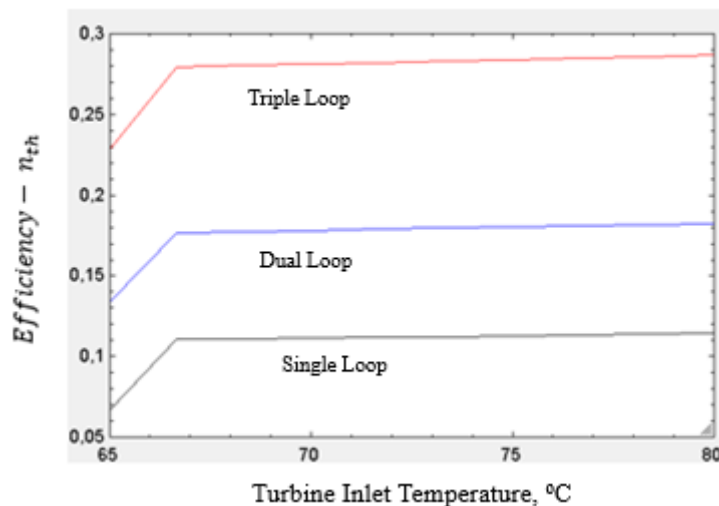


Figure 3. Variation the energy efficiency versus Turbine-1 inlet temperature for R290.

According to Fig. 3, the efficiency ranges between 6% and 11% for the single looped system. It ranges between 13.5% and 18% for dual looped system where it ranges between 23% and 28% for triple looped system. According to the obtained results, the optimum configuration was determined for 66.5 °C where a sharp breaking point was observed considering the economical factors. Fig. 4 shows the cycle efficiencies according to the variation of the turbine inlet pressure (P_3).

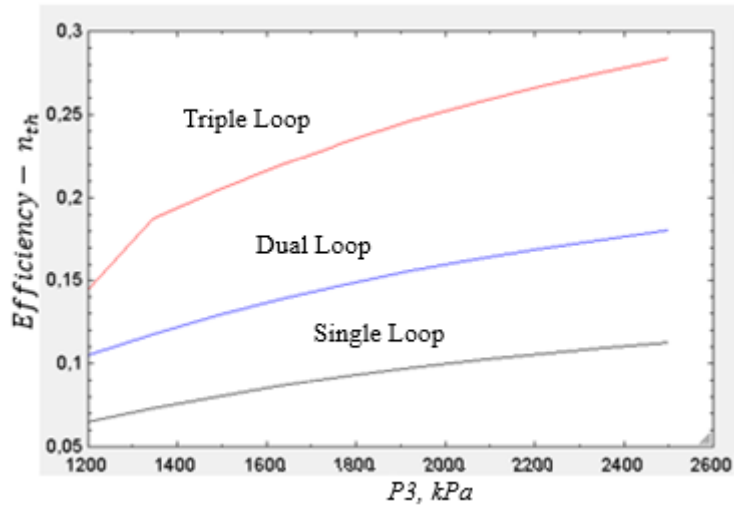


Figure. 4. Variation the energy efficiency versus P_3 for R290 ($T_3=80$ °C).

According to Fig. 4, the efficiency ranges between 6.5% and 11% for the single looped system. It ranges between 10.5% and 17.0% for dual looped system where it ranges between 14.5% and 28.4% for triple looped system. According to the obtained results, the optimum configuration was determined for 2500 kPa which is the available maximum.

3.3. The Case of Using R290 in the First Cycle and R22 in the Second and Third Cycles

In the second stage of the analysis, the calculations were made by using the most efficient fluid of R290 in single, and R22 dual and triple looped cases. First, the ORC with single loop is evaluated. Then, dual and triple looped cases were handled. For the turbine inlet temperature of the loops, a temperature difference of 5 °C was taken into account. The inlet pressure was taken as 2500 kPa. Fig. 5 shows the cycle efficiencies according to the variation of the turbine inlet temperature (T_3).

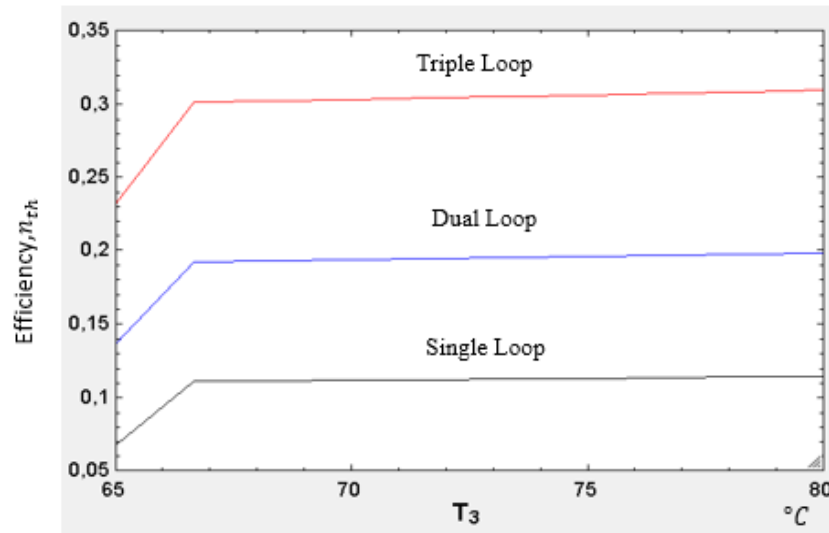


Figure 5. Variation the energy efficiency versus T_3 for fluid of R290 single loop and fluid of R22 dual and triple loop.

According to Fig. 5, the efficiency ranges between 7% and 11% for the single looped system. It ranges between 14% and 19% for dual looped system where it ranges between 23.5% and 30.5% for triple looped system. According to the obtained results, the optimum configuration was determined for 66.8 °C again where a sharp breaking point was observed considering the economical factors. Fig. 6 shows the cycle efficiencies according to the variation of the turbine inlet pressure (P_3).

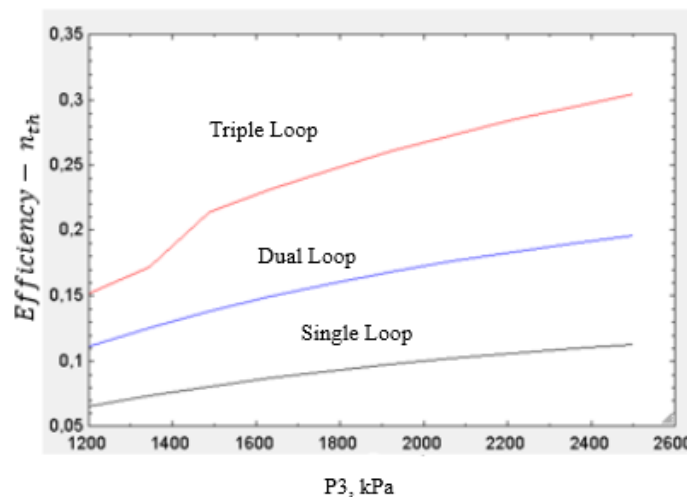


Figure 6. Variation the energy efficiency versus P_3 for single loop R290 and fluid of R22 for dual and triple loop ($T_3=80$ °C).

According to Fig. 6, the efficiency ranges between 6.5% and 11% for the single looped system. It ranges between 11% and 17% for dual looped system where it ranges between 15% and 30.5% for triple looped system. According to the obtained results, the optimum configuration was determined for 2500 kPa which is the handle maximum.

3.4. The Case of Using R290 in the First Cycle, R22 in the Second Cycle, and R123 in the Third Cycle

In the final stage of the analysis, the calculations were made by using the most efficient fluid of R290 in single, R22 in dual and f R123 in triple looped cases. First, the ORC with single loop is evaluated. Then, dual and triple looped cases were handled again. The inlet pressure was taken as 2500 kPa. Fig. 7 shows the cycle efficiencies according to the variation of the turbine inlet temperature (T_3).

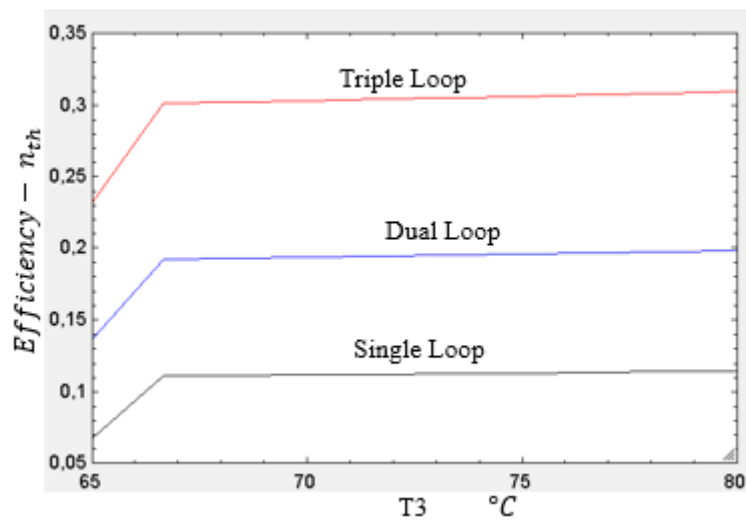


Figure 7. Graphic of the calculation results for three different fluid and parametric temperatures

According to Fig. 7, the efficiency ranges between 7% and 11.5% for the single looped system. It ranges between 14% and 20% for dual looped system where it ranges between 23.5% and 31% for triple looped system. According to the obtained results, the optimum configuration was determined for 66.8 °C where a sharp breaking point was observed considering the economical factors as in the other cases. Fig. 8 shows the cycle efficiencies according to the variation of the turbine inlet pressure (P_3).

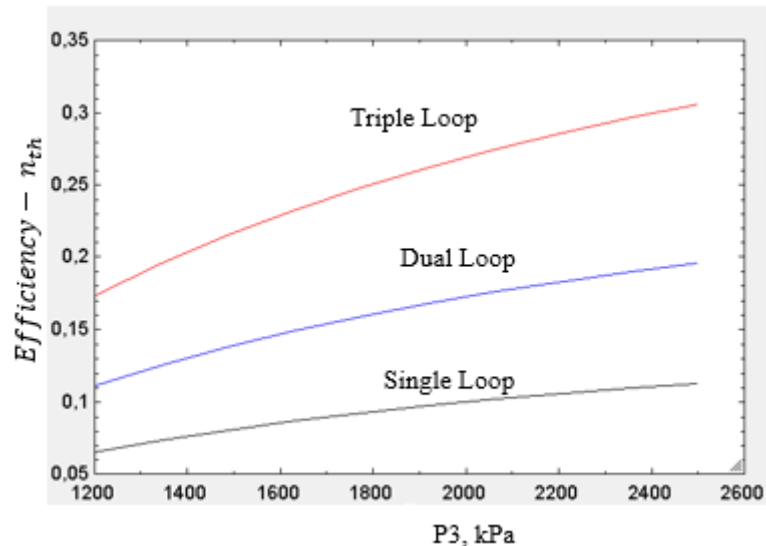


Figure 8. Graphic of the calculation results in three different fluid and parametric pressure conditions.

According to Fig. 8, the efficiency ranges between 6.5% and 11% for the single looped system. It ranges between 11% and 18% for dual looped system where it ranges between 17.5% and 31% for triple looped system. According to the obtained results, the optimum configuration was determined for 2500 kPa which is the handle maximum.

Although simple one-cycle Rankine cycles are the most frequently used systems, the use of two or more cycle systems has increased recently. As can be seen in this study, when the number of cycles increased to two as a result of the analyzes made with the EES software. the efficiency increased significantly. Since the cost of each cycle is significant, the decision should be made after the economic evaluation for two or three looped systems. One of the main aims of the study is to understand the effect of the fluids used on efficiency. When the same fluid (R290) is used in each cycle, the maximum efficiency is 29% for parametric temperature and pressure. When two different fluids are used, it is 30%. Finally for the different fluids in each loop, it is 31%. The thermo-physical properties of the best design are given in Table7.

Table 7. Thermo-physical properties of the best ORC design.

Points	Fluid	m (kg/s)	T (°C)	P (kPa)	h (kJ/kg)	S (kJ/kgK)	ψ	Ex
0	Stack gases	-	25	100	309.3	6.839	-	-
0	R290	-	25	100	630.8	2.849	-	-
0	R22	-	25	100	429.3	1.984	-	-
0	R123	-	25	100	226.2	1.091	-	-
0	Water	-	25	100	104.8	0.3669	-	-
1	R290	6.55	27	925	271	1.226	1392	58089
2	R290	6.55	28.2	2758	387.8	1.75	3023	126153

3	R290	6.55	80	2500	691.9	2.408	5169	215707
4	R290	6.55	48.34	971.6	644.3	2.408	4629	193172
5	R22	15.44	22	1960	226.6	1.129	1144	572447
6	R22	15.44	80	2500	448.8	1.709	2975	1488663
7	R22	15.44	33.43	596.2	422.4	1.709	2594	1298014
8	R22	15.44	20	584.3	225.4	1.026	8596	430136
9	R22	15.44	21.59	2000	229.7	1.217	1402	701548
10	R123	61.08	18	980	219.2	1.204	1362	2261032
11	R123	61.08	75	2500	285.9	1.242	1481	2458581
12	R123	61.08	10.48	369.5	276.1	1.242	140	2324115
13	R123	61.08	10	362.1	210.8	1.011	8205	1362097
14	R123	61.08	12.5	1000	213.3	1.014	8357	1387331
15	Stack gases	32.61	207	120	495.5	3.496	2566	975080
16	Stack gases	32.61	148.5	120	433.7	3.282	2201	836380
17	Stack gases	32.61	119.3	120	401	7.033	1211	460180
18	Stack gases	32.61	89.7	120	381	6.99	1066	405080
19	Water	6.18	-5	100	-343.4	-1.259	-4076	-1223615
20	Water	6.18	7	100	301.8	0.01066	-929	-278886

According to values given in Table 7, the results of exergy analysis on the component basis are given in Table 8.

Table 8. Exergy analysis results of the best ORC design.

Components	Q (kW)	W	Eg	Ec	Exg	Exc	Exd	η (%)	E (%)
E-1	1991.62	-	485066.92	733256.02	331980.37	562488.74	171821.53		
T/G-1	-	265.01	733256.02	674942.56	562488.74	504175.28	49571.93		
C-1	1680.07	-	674942.56	291567.28	504175.28	291567.28	166045.09		
P-1	-	25.43	291567.28	485066.92	291567.28	331980.37	34622.38		
Loop-1	311.55	239.58						11%	12%
HE-1	994.11		1505180.00	1485420.00	830680.00	460180.00	-387789.82		
T/G-2		346.47	571367.40	521855.04	389383.13	339739.08	42138.18		
C-2	47.86		521855.04	272976.40	339739.08	113193.69	22333.24		
P-2		30.88	272976.40	352380.54	113193.69	184617.91	69676.80		
Loop-2	946.24	315.6						31%	44%
HE-2	1029.52		1485420.00	1428040.00	454100.00	402800.00	-78901.05		
T/G-3		508.80	119788.02	116293.11	64437.39	60986.17	2951.89		
C-3	152.71		116293.11	88683.33	60986.17	35844.67	2284.80		
P-3		152.7	88683.33	89382.31	35844.67	36508.70	338.31		
Loop-3	876.81	356.1						34%	48%
Overall	2134.6	911.28						23%	34%

According to Table 8, the highest exergy destruction was occurred in E-1 with a value of 1991.62 kW in Loop-1; P-2 with a value of 30.88 kW in LOOP-2 and T/G-3 with a value of 508.8 kW in LOOP-3. The energy and exergy efficiencies of Loop-1 were determined as %11 and %12 respectively. The energy and exergy efficiencies of Loop -2 were determined as %31 and %44, respectively. The energy and exergy efficiencies of Loop -3 were determined as %34 and %48. For the overall system, the energy and exergy efficiencies were determined as % 23 and %34 respectively.

4. CONCLUSION

In this study the organic Rankine cycle with multi-loop was analyzed by energy and exergy method. EES software was used in the calculations. The waste heat of a ceramic factory was evaluated for this purpose to reduce energy costs.

One of the main aims of the study is to understand the effect of the fluids used on efficiency. In the analysis, the maximum efficiency is 29% when the same fluid (R290) is used in each cycle. It is 30% if two different fluids are used. It is 31% if different types of fluids are used in each loop. This means that using different types of fluid in each loop gives the most efficient result.

The results obtained showed that the efficiency increases with the increase of loop number. However, it is issue that the initial investment cost of each loop corresponds to significant amounts. So, it is necessary to handle an economic evaluation.

ACKNOWLEDGMENT

This research received no specific grants from any funding agency in public, commercial or non-profit sectors.

REFERENCES

- [1] Tchanche, B., Lambrinos, G., Frangoudakis, A. and Papadakis, G. (2011), Low-Grade Heat Conversion Into Power Using Organic Rankine Cycles-A Review of Various Applications Renewable and Sustainable Energy Reviews vol 15 no 8 pp 3963-3979.
- [2] Arslan, O., Ozgur, M.A. and Kose, R. (2012), Electricity generation ability of Simav geothermal field: A technoeconomic approach. Energy Sources, Part A, 34: 1130– 1144.
- [3] Boukelia, T.E., Arslan, O., Bouraoui, A., (2021), Thermodynamic performance assessment of a new solar tower-geothermal combined power plant compared to the conventional solar tower power plant, Energy, Volume 232, 121109.
- [4] Arslan, O., Erbas, O., Ozgur, M.A. and Kose, R. (2012), ANN based optimization of b2 and b3 types of ORC-Binary geothermal power plant: Simav case study. Energy Education Science and Technology Part A: Energy Science and Research, 28(2): 1039–1050.

- [5] Arslan, O. (2015), ANN Approximation of Geothermal Aided Power Cycles Energy Sci. and Tech. Vol. 9: Geothermal and Ocean Environment, Chapter 7., pp: 163-188. Studium Press LLC, USA.
- [6] Arslan, O. and Yetik, O. (2014), ANN modelling of ORC-binary geothermal power plant: Simav case study. Energy Sources, Part A, 36: 418–428.
- [7] Arslan, O. , Ergenekon Arslan, A. and Şentürk Acar, M. (2019), Multi-Criteria Making-Decision Modeling of b-type ORC-Binary Geothermal Power Plant: EATWOS Analysis . Bilecik Şeyh Edebali Üniversitesi Fen Bilimleri Dergisi , 6 (1) , 29-48 . DOI: 10.35193/bseufbd.561668.
- [8] Arslan, A.E., Arslan, O. and Kandemir, S.Y. (2021), AHP–TOPSIS hybrid decision-making analysis: Simav integrated system case study. J Therm Anal Calorim 145, 1191–1202
- [9] Arslan, A.E, Senturk, M.A, Arslan, O. (2018), Effectiveness analysis of orc-binary geothermal power plant using data enveloping. Proceedings of International Congress ON Afro-Eurasian Research IV, pp: 109-117, April 27-29, 2018, Budapest, Hungary.
- [10] Arslan, A.E, Senturk, M. A, Arslan, O. (2018), Data enveloping based effectiveness analysis of integrated geothermal system: Simav case study. Proceedings of International Congress ON Afro-Eurasian Research IV, pp: 118-124, April 27-29, 2018, Budapest, Hungary.
- [11] Arslan,, O., Kılıç D., (2021), Concurrent optimization and 4E analysis of organic Rankine cycle power plant driven by parabolic trough collector for low-solar radiation zone, Sustainable Energy Technologies and Assessments, Volume 46, 101230.
- [12] Erikgenoğlu, D., Arslan O., (2021), Artificial neural network modelling of parabolic trough types solar thermal power plant, Turkish Journal of Electromechanics and Energy Vol 6, No 3
- [13] Varga, Z., Varga, R., Istvan, C. and Farkas C., (2012), Waste Heat Recovery with Organic Rankine Cycle in the Petroleum Industry Researchgate
- [14] Chen, C., Li, P., Le, S., (2016), Organic Rankine Cycle for Waste Heat Recovery in a Refinery American Chemical Society
- [15] Arslan, O., Acikkalp, E., Genç, G.,(2022), A multi-generation system for hydrogen production through the high-temperature solid oxide electrolyzer integrated to 150 MW coal-fired steam boiler Fuel, Volume 315, 123201, ISSN 0016-2361.
- [16] Arslan, O., (2021), Performance analysis of a novel heat recovery system with hydrogen production designed for the improvement of boiler effectiveness, International Journal of Hydrogen Energy, Volume 46, Issue 10, 7558-7572.
- [17] Arslan, O., Yetik, O., (2011), ANN based optimization of supercritical ORC-Binary geothermal power plant: Simav case study, Applied Thermal Engineering , 2011 , 31 , 17-18 , 3922-3928

- [18] Hung, T. (2001), Waste heat recovery of organic Rankine cycle using dry fluids, *Energy Conversion and Management*, Volume 42, pp:539-553
- [19] Ouyang, T., Su, Z., Huang, G., Zhao, Z., Wang, Z., Chen, N. and Huang, H., (2019), Modeling and Optimization of a Combined Cooling Cascaded Power and Flue Gas Purification System in Marine Diesel Engines. *Energy Conversion and Management*, 151, pp:286-295.
- [20] Sciubba, E., Tocci, L., Toro, C., (2016), Thermodynamics Analysis of a Rankine Dual Loop Waste Thermal Energy Recovery System, *Energy Conversion and Management*, 122, pp: 109-118, 2016.
- [21] Braimakis, K. and Karellas, S., (2018), Exergetic Optimisation of double stage Organic Rankine Cycle (ORC), *Energy*, 2018. doi: 10.1016/j.energy.2018.02.044.
- [22] Xia, X., Wang, Z., Zhou, N., Hu, Y., Zhang, J. and Chen, Y., (2020), Working Fluid Selection of Dual-Loop Organic Rankine Cycle Using Multi-Objective Optimization and Improved Grey Relational Analysis, *Applied Thermal Engineering*, 171.
- [23] Ceylan, I. (2022), Design and Optimization of Staged ORC Power Plant by Waste Heat. Unpublished Master's Thesis, University of Bilecik Şeyh Edebali, Turkey.
- [24] Kavasogulları. B. and Han. E. (2015), Organik Rankine Çevrimi (ORC) ile Birlikte Çalışan Buhar Sıkıştırılmalı Bir Soğutma Çevriminin Ekserji Analizi. *Tesisat Mühendisliği*. P.150.
- [25] He, C., Liu, C., Gao, H., Xie, H., Li, Y., Wu, S., (2012), The optimal evaporation temperature and working fluids for subcritical organic Rankine cycle. *Energy*, 38, 136-143.
- [26] Lai, N.A, Wendland, M, Fischer J., (2011), Working fluids for high-temperature organic Rankine cycles. *Energy*, 36, 199-211.
- [27] Sauret, E, Rowlands, A.S., (2011), Candidate radial-inflow turbines and high-density working fluids for geothermal power systems. *Energy*, 36, 4460-4467.
- [28] Nouman, J. (2012), Comparative studies and analyses of working fluids for Organic Rankine Cycle-ORC, KTH Industrial Engineering and Management, Master of Science Thesis, Stockholm, pp 83-87, 2012
- [29] Çengel, Y. and Boles, M. (2012), *Thermodynamics: An Engineering Approach* 5 Edition.

NOMENCLATURE

C-1	:	Condenser-1
C-2	:	Condenser-2
C-3	:	Condenser-3
E	:	Exergy Efficiency
E-1	:	Evaporator-1

Ec	:	Energy outlet		
Eg	:	Energy inlet		
EES	:	Engineering Equation Solver		
Exc	:	Exergy outlet		
Exd	:	Exergy		destruction
Exg	:	Exergy inlet		
GWP	:	Global	Warming	Potential
h	:	Enthalpy		
HE-1	:	Heat Exchanger-1		
HE-2	:	Heat Exchanger-2		
ODP	:	Ozone Depletion Potential		
P	:	Pressure		
P-1	:	Pump-1		
P-2	:	Pump-2		
P-3	:	Pump-3		
Q	:	Heat Energy		
s	:	Entropy		
T	:	Temperature		
T/G-1	:	Turbine/Generator-1		
T/G-2	:	Turbine/Generator-2		
T/G-3	:	Turbine/Generator-3		
W	:	Work		
η	:	Efficiency		